

## Inhibition of carbonate synthesis in acidic oceans on early Mars

Alberto G. Fairén<sup>1</sup>, David Fernández-Remolar<sup>2</sup>, James M. Dohm<sup>3</sup>, Victor R. Baker<sup>3,4</sup> & Ricardo Amils<sup>1,2</sup>

<sup>1</sup>Centro de Biología Molecular, CSIC–Universidad Autónoma de Madrid, 28049-Cantoblanco, Madrid, Spain

<sup>2</sup>Centro de Astrobiología (CSIC–INTA), 28850-Torrejón de Ardoz, Madrid, Spain

<sup>3</sup>Department of Hydrology and Water Resources, <sup>4</sup>Lunar and Planetary Laboratory, University of Arizona, Tucson, Arizona 85721, USA

Several lines of evidence have recently reinforced the hypothesis that an ocean existed on early Mars<sup>1–7</sup>. Carbonates are accordingly expected to have formed from oceanic sedimentation of carbon dioxide from the ancient martian atmosphere<sup>7,8</sup>. But spectral imaging of the martian surface has revealed the presence of only a small amount of carbonate, widely distributed in the martian dust<sup>9</sup>. Here we examine the feasibility of carbonate synthesis in ancient martian oceans using aqueous equilibrium calculations. We show that partial pressures of atmospheric carbon dioxide in the range 0.8–4 bar, in the presence of up to 13.5 mM sulphate and 0.8 mM iron in sea water<sup>8</sup>, result in an acidic oceanic environment with a pH of less than 6.2. This precludes the formation of siderite, usually expected to be the first major carbonate mineral to precipitate<sup>8</sup>. We conclude that extensive interaction between an atmosphere dominated by carbon dioxide and a lasting sulphate- and iron-enriched acidic ocean on early Mars is a plausible explanation for the observed absence of carbonates.

A survey of the literature suggests four alternative classical explanations for the detection of only small concentrations of carbonate minerals: (1) no primary carbonate formation in a cold and/or dry environment; (2) the inability of the Thermal Emission Spectrometer (TES; on board the Mars Global Surveyor spacecraft) and the Thermal Emission Imaging System (THEMIS; on board the Mars Odyssey spacecraft) to detect carbonates; (3) secondary chemical alteration of ancient carbonate sediments; or (4) carbonates that are obscured by younger rock materials. The first explanation, which is in disagreement with the geomorphological evidence, supports the interpretation of early martian conditions as having been similar to those prevailing at present<sup>10</sup>. The second highlights the possibility that substantial regional carbonate deposits can be 100% exposed and remain undetected at the sensitivity of TES/THEMIS<sup>11</sup>. The third includes the possibility of water vapour and sulphates combining to form acid rain<sup>4</sup> and thereby promoting chemical decomposition of superficial carbonate layers, acid-fog weathering<sup>12</sup>, and/or photodecomposition<sup>13</sup>. And the fourth includes large carbonate deposits hidden beneath several-centimetres-thick secondary alteration rinds that envelop rock materials on the surface<sup>14</sup>, or carbonates masked by the formation of relatively recent volumetrically abundant soils<sup>14</sup>; it also includes other resurfacing processes that may have mantled carbonate deposits, such as eolian deposition during the dominant phases of Mars' mostly frozen state<sup>15</sup>, sedimentation in a later Hesperian-age ocean that occupied the northern plains<sup>5</sup>, emplacement of basaltic lavas and pyroclastic materials in and around the Tharsis and Elysium magmatic complexes<sup>3</sup>, and the deposition of 100-m-thick Vastitas Borealis Formation materials, a potentially ice-rich sublimation residue of outflow events<sup>16</sup>.

Using aqueous equilibrium calculations, we analyse here the feasibility of carbonate synthesis in ancient martian oceans, taking into account the geochemical cycles that were probably in operation then. To this end, our analysis is based on two key assumptions: (1)

that well over 90% of the carbonate rock formation on Earth occurs in open bodies of liquid water<sup>17</sup>; and (2) that the fate of the martian oceans was rapid freezing solid followed by sublimation and cold-trapping of ice at higher latitudes<sup>1,10</sup>. Thus, the problem of carbonate formation on early Mars basically concerns the chemical conditions operating in open bodies of liquid water. Local sedimentation driven by sequential evaporation in closed basins<sup>8</sup> is considered here an interesting, but minor, mode of water evolution on early Mars; and where such processes are likely to have occurred, the subsequent increase of iron and sulphate in the solution would have further lowered the pH, thus maintaining ionic undersaturation with respect to carbonates. On the other hand, more recent transitory reduced lakes would not have been able to control the process of carbonate synthesis either, as Mars has been mainly cold and dry throughout the Hesperian and the Amazonian, except during brief and intriguing episodes<sup>5,15</sup>.

To raise the mean surface temperature of Mars above the freezing point, a greater atmospheric CO<sub>2</sub> pressure is required. The present CO<sub>2</sub> pressure (6 mbar), in addition to that adsorbed in the regolith (30–40 mbar; ref. 18) and the minimum quantity sequestered as ice or clathrate in the poles, represent nearly 40 mbar of CO<sub>2</sub>. If the elimination processes by impact erosion and pick-up ion sputtering removed 95–99% of the Noachian atmosphere<sup>18</sup>, then the martian surface CO<sub>2</sub> pressures 4 Gyr ago could have been of the order of 800–4,000 mbar. However, without the additional warming provided by the presence of other strong greenhouse gasses, such as CH<sub>4</sub> and NH<sub>3</sub> (ref. 19), even 4 bar of CO<sub>2</sub> would have been insufficient to yield mean global temperatures above the freezing point. Carbon dioxide ice clouds in the troposphere may have also contributed to warming early Mars, as ice particles reflect the outgoing thermal infrared radiation back to the surface<sup>20</sup>.

Nevertheless, this approach for high CO<sub>2</sub> pressures in early Mars has been classically disputed by two lines of arguments: the loss of atmospheric volatiles<sup>18</sup>, and the lack of carbonates on the martian surface<sup>10</sup>. But substantial amounts of atmospheric CO<sub>2</sub> may have been maintained during the Noachian by volcanic outgassing from Tharsis<sup>2,3,5</sup>. In addition, if the oceans were acidic, the lack of carbonates no longer qualifies as a reliable indicator of CO<sub>2</sub> partial pressures in the Noachian martian atmosphere. Consequently, the possibility of substantial atmospheric CO<sub>2</sub> pressures in early Mars cannot be ruled out. Later, nearly all of the martian atmosphere would have been lost by impact erosion during the heavy bombardment period<sup>18,21</sup>, and by sputtering acting throughout most of the martian history<sup>18</sup>.

Such a carbon dioxide-dominated atmosphere in early Mars would have rendered an ocean mildly acidic by releasing free protons in the sequence  $\text{H}_2\text{O} + \text{CO}_2(\text{g}) \leftrightarrow \text{H}_2\text{CO}_3 \leftrightarrow \text{H}^+ + \text{HCO}_3^-$ . The addition of iron contributed even more to oceanic acidification. Also, sufficient iron in solution acted as an excellent buffer, as appreciable amounts of iron can be dissolved in moderately acidic to neutral solutions. Hydrolysis of ferrous iron generates free protons by the equilibrium  $\text{Fe}^{2+} + 2\text{H}_2\text{O} \leftrightarrow \text{Fe}(\text{OH})_2 + 2\text{H}^+$ , and the process is much more effective if the iron is in the form of ferric iron:  $\text{Fe}^{3+} + 3\text{H}_2\text{O} \leftrightarrow \text{Fe}(\text{OH})_3 + 3\text{H}^+$ .

The potential source of iron in terrestrial Archaean oceans was iron emitted from hydrothermal vent fluids produced by intense submarine magmatic activity creating hot Fe<sup>2+</sup>-enriched plumes<sup>22</sup>; and the subsequent photolytic oxidation of ferrous iron to Fe<sup>3+</sup> would provide the ocean with its major oxidized species<sup>23</sup>. Consequently, iron is thought to have been abundant in the oceans of early Earth, reaching concentrations as high as 50 μM (ref. 24). On early Mars, the iron-rich nature of the mantle and active volcanism<sup>3</sup> produced igneous minerals containing ferrous iron. In fact, the martian surface is much richer in iron than the surface of Earth: the reddish colour of the martian surface is due to the optical properties of ferric-iron-bearing minerals present in the oxidized surface layer<sup>25</sup>. In this sense, up to 800 μM of Fe<sup>2+</sup> for basin feedwater<sup>8</sup>

on the surface of early Mars has been considered a reasonable estimate for an iron-rich fluid.

Moreover, jarosite minerals, as well as evaporite deposits containing magnesium sulphate salts, a typical sublimation residue, have been detected by the Mars Exploration Rover (MER) Opportunity in the sediments deposited at Meridiani Planum. The amount of salts detected, up to 40% in the outcrop<sup>7</sup>, leads us to expect that sulphate levels in ancient martian oceans were at least at the same order of magnitude as those derived from weathered ultramafic rocks on Earth (0.18 mM; ref. 8), since the salinity of present-day terrestrial oceanic water is  $3.5 \times 10^5$  p.p.m. (ref. 26). Following the Opportunity results, however, we assume a  $\text{Fe}^{3+}$ -enriched solution in equilibrium with jarosite<sup>27</sup> at least locally and/or temporarily, so potentially displaying even higher sulphate levels, up to 13.5 mM (see Table 1).

For the Noachian oceans, aqueous thermodynamic calculations considering a solution enriched in iron hydroxides and sulphate result in a pH between 5.3 and 6.2 for the siderite- $\text{Fe}^{2+}$  equilibrium; and when the ferrous iron was photolytically oxidized to ferric, the final pH was between 1.9 and 2.1 for the siderite- $\text{Fe}^{3+}$  equilibrium (Fig. 1; see Methods). The subsequent evolution of the acidic environment over time results in  $\text{Fe}^{3+}$ -sulphatic species dominating the chemistry of the oceans (Fig. 2). Thus, the TES analyses, which indicate an absence of carbonate minerals at the surface of Mars, can be comprehensively explained by the acidity of the ancient martian oceans. These results address the recently posed contradiction between TES-detected martian mineralogy, and planetary geomorphology and MER-unveiled geochemistry, the former reporting small amounts of disseminated carbonates and the latter evidencing the geomorphologic modification and chemical alteration of surface materials through significant amounts of running water during long periods of early Mars history. Also, this new scenario is qualitatively different from all those argued before (and listed above), as they account for masking or altering the carbonates actually synthesized in a reducing environment. On the contrary, in our model, carbonate rock layers simply never formed, but instead we envisage the possibility of a warmer and wetter Mars, where extensive interaction between significant amounts of moderate to extreme acidic liquid water and a  $\text{CO}_2$  atmosphere might have occurred (Fig. 3).

The viability of the model proposed here for ancient Mars is supported by the latest observational evidence provided by MER Opportunity at Meridiani Planum. Also on the modern Earth, the headwaters of the Tinto river system (in the southwest of Spain), an extreme acidic environment controlled by iron biogeochemistry, produces ferric-iron-enriched sediments dominated by sulphate and oxihydroxide parageneses, resulting in goethite, haematite and jarosite, analogous to the minerals found in Meridiani<sup>28</sup>. In the living Tinto river system, the values of pH, redox potential, and

Table 1 Assumed average composition for surface waters on early Mars

Constituent	Concentration (p.p.m.)	Molality ( $\times 10^{-3}$ mol kg <sup>-1</sup> )	Activity
$\text{SiO}_2(\text{aq})$	10.8–60.1	0.18*–1.0	$10^{-3.75}$ – $10^{-3}$
$\text{Fe}^{2+}/\text{Fe}^{3+}$	3–44.7	0.05†–0.8	$10^{-4.3}$ – $10^{-3.1}$
$\text{SO}_4^{2-}$	17.3 (624–1,263)	0.18 (6.5–13.5)‡	$10^{-3.745}$ ( $10^{-2.19}$ – $10^{-1.88}$ )
$\text{Mg}^{2+}$	24.3	1.0	$10^{-3}$
$\text{Cl}^-$	23.0	0.65	$10^{-7}$
$\text{Ca}^{2+}$	20.0	0.5	$10^{-3.19}$
$\text{Na}^{2+}$	18.4	0.8	$10^{-3.1}$
$\text{K}^+$	2.7	0.07	$10^{-4.16}$

Concentration and molality data after ref. 8, except as shown by footnote symbols as follows.

\*From ref. 30.

†From ref. 24.

‡Obtained assuming a solution at 273 K in equilibrium with jarosite for  $a_{\text{Fe}^{3+}} = 10^{-4.3}$  and  $a_{\text{Fe}^{2+}} = 10^{-3.1}$ , respectively, as governed by the equation  $\log a_{\text{SO}_4^{2-}} = 3\log a_{\text{H}^+} - 0.5\log a_{\text{K}^+} - 1.5\log a_{\text{Fe}^{3+}} - 2.91$ .

$\text{HCO}_3^-$  is not a fixed parameter here, as it has been swapped for  $\text{CO}_2(\text{g})$ , the y-axis variable in Fig. 1a.

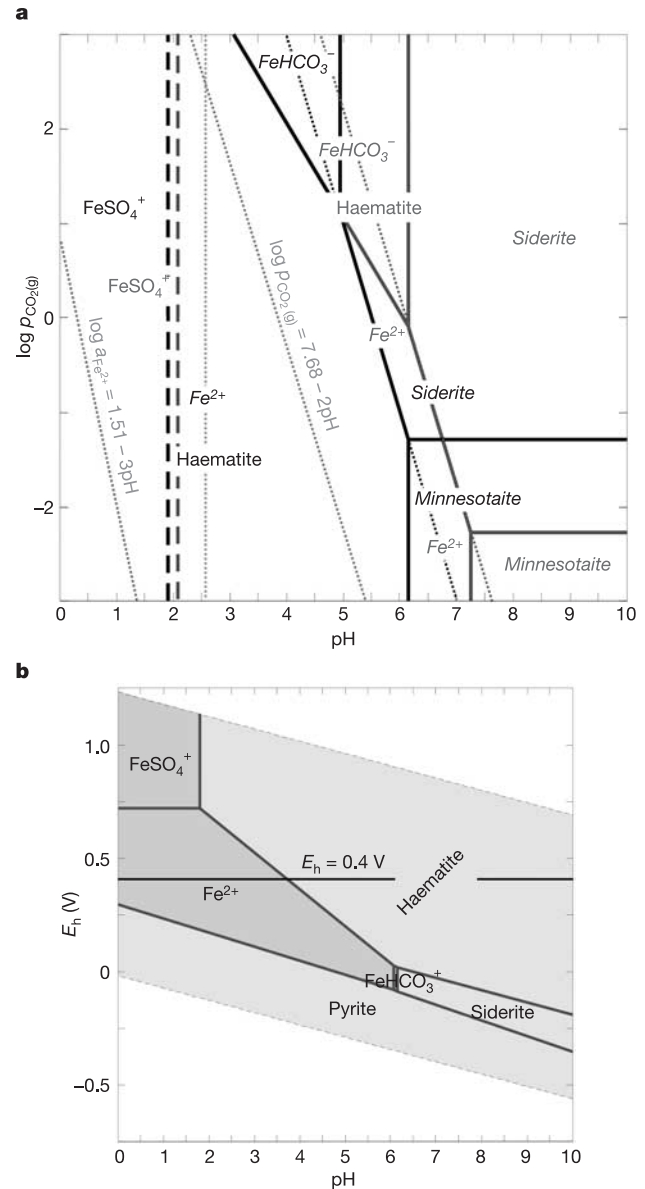


**Figure 1** Stability boundaries of siderite and minnesotaite (under reducing conditions) and acidic solutions and haematite (under oxidizing conditions) on early Mars. **a**, Stability boundaries obtained as a function of  $\text{CO}_2$  pressure and pH, calculated at 273 K for four different solutions: black lines represent a solution containing Fe and  $\text{SiO}_2(\text{aq})$  at their upper limits (800  $\mu\text{M}$  and 1 mM, respectively); grey lines represent the lower limits assumed here (50  $\mu\text{M}$  and 180  $\mu\text{M}$ ); solid lines represent reducing conditions ( $\text{Fe}^{2+}$ ) and standard  $[\text{SO}_4^{2-}] = 0.18$  mM; and dashed lines represent oxidizing conditions ( $\text{Fe}^{3+}$ ) and upper and lower limits for  $[\text{SO}_4^{2-}] = 6.5$  (black) and 13.5 (grey) mM, driving to the formation of haematite and acidic solutions from which jarosite is expected to form at  $\text{pH} \approx 2$  (boundary of jarosite stability). Dotted lines represent, from left to right: (1) the pH buffer when  $\text{Fe}^{3+}$  controls the solution, under acidic and oxidizing conditions, assuming goethite as the ultimate chemical product ( $\text{Fe}^{3+} + \text{H}_2\text{O} \leftrightarrow \text{FeOOH}(\text{goethite}) + 3\text{H}^+$ ); (2) the equilibrium pH of jarosite ( $(\text{K}_2\text{Fe}_6(\text{SO}_4)_4(\text{OH})_{12}) + 6\text{H}^+ \leftrightarrow 2\text{SO}_4^{2-} + 6\text{H}_2\text{O} + \text{K}^+ + 3\text{Fe}^{3+}$ ) when minimum values for  $\text{Fe}^{3+}$  (50 mM) and sulphates (180 mM) are considered; (3) the changes in pH exclusively controlled by the  $p_{\text{CO}_2}$ ; and (4 and 5) the relationship between  $\text{CO}_2$  pressure and pH for each modelled solution ( $\text{pH} = 5.6 - 0.5\log p_{\text{CO}_2}$  and  $\text{pH} = 6.1 - 0.5\log p_{\text{CO}_2}$ , respectively). All constituents included in the solutions for displaying this graphic are quantified in Table 1. **b**,  $E_{\text{h}}$ -pH diagram assuming the lower values of Table 1, at  $p_{\text{CO}_2} = 1$  atm and  $T = 273$  K. The stability fields of jarosite (acidic oxidizing solutions with  $\text{FeSO}_4^+$ ), haematite and siderite are represented. Dark grey indicates phase solutions, while light grey indicates minerals. Jarosite formation is favoured by  $E_{\text{h}} > 0.4$  V and  $\text{pH} < 2$ .

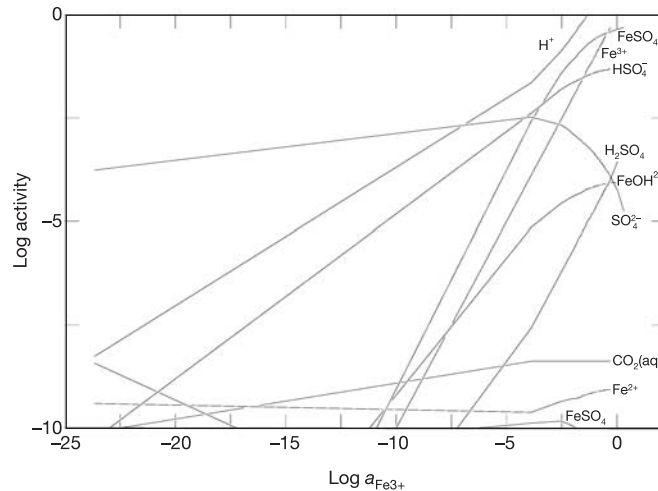


**Figure 2** Evolution of the acidic martian environment over time. Evolution of solution and gas compositions, starting from an initial pH = 7 and  $E_h = 0.4$  V, at increasing concentration of  $\text{Fe}^{3+}$  and  $\text{H}_2\text{SO}_4$ .  $\text{Fe}^{3+}$  concentration ranges from  $1.4 \times 10^{-5}$  M to 0.5 M, a current record in modern acidic waters at the Tinto river<sup>28</sup>. Although the ferric ion can acidify different solutions when added at high concentrations, sulphuric solutions generated by  $\text{H}_2\text{S}$  and  $\text{SO}_2$  photo-oxidation may indeed generate acidic conditions at first, acting as an acidic matrix for later reactions that produce jarositic associations after

evaporation. Thus, the system has been coupled to an increased concentration of  $\text{H}_2\text{SO}_4$  from the initial equilibrium to  $10^{-4}$  M, a rough estimation for the acidic waters of the Tinto river<sup>28</sup>. Although a high diversity of chemical species emerged, following the MER Opportunity results only S and Fe species are displayed, that is, those that would dominate the hypothetical chemistry of the early martian oceans. In this case,  $\text{Fe}^{3+}$ –sulphatic species would favour the ferric sulphate precipitation.

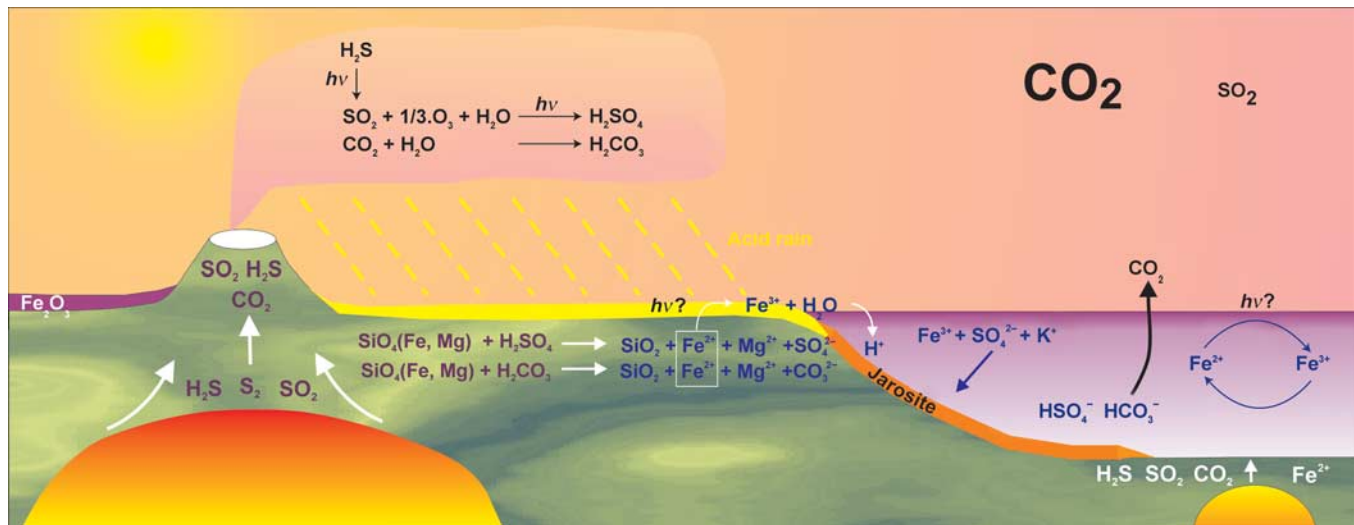


**Figure 3** Schematic representation of atmosphere–land–ocean interactions generating acidic environments in early Mars. The acidic attack of ultramafic crust is driven by  $\text{H}_2\text{SO}_4$  (generated by volcanic  $\text{SO}_2$  photolysis) and  $\text{H}_2\text{CO}_3$ , and consequently weathering of basalt releases Fe and Mg to the sea water. As ferrous iron oxidizes to ferric,  $\text{Fe}^{3+}$  drives the water more and more acidic, as also does  $\text{SO}_2$  forming dilute sulphuric acid. From these solutions, jarosite as well as Mg sulphates are expected to precipitate, as highlighted by

MER Opportunity at Meridiani. Also, the acidic weathering process would generate a sulphate layer over the basaltic crust, potentially able to evolve to haematite by dehydration of the ferric sulphates and related iron-bearing minerals. Under such conditions,  $\text{HCO}_3^-$ , the main source of carbonates, is at very low concentration, and therefore all C is expected to be in the form of  $\text{CO}_2(\text{aq})$  and  $\text{CO}_2(\text{g})$ , with higher residence time in the atmosphere and therefore maintaining long-term milder surface temperatures.

$\text{Fe}^{3+}$  and sulphate concentration remain constant in different years under variable rain regimes. Life is highly diverse in the Tinto system, allowing us to suggest comparable ancient acidic aquatic habitats hosting a putative early biosphere on Mars. In fact, if biological inhabitation of early Mars is considered plausible, moderate acidic oceans represent the closest terrestrial analogue for a biogenic environment, similar to that where life originated on the Hadean–Early Archaean Earth<sup>23,26</sup>. In the Tinto river system, the remobilization of iron and its subsequent precipitation as ferric

minerals preserves biological remains sometimes in remarkable detail, suggesting an analogous record in the rock exposures derived from the acidic martian early environments. □

**Methods**

We use the values listed in Table 1 to estimate limits on the pH and composition of the putative Noachian ocean, which includes considering the addition of supplementary cations such as  $\text{Mg}^{2+}$ ,  $\text{Ca}^{2+}$ ,  $\text{K}^+$  or  $\text{Na}^+$ , and silica (a by-product of the acid dissolution of ferromagnesian silicates, typical of martian igneous rocks in such acidic oceans), as they are effective solutes that raise the pH (ref. 8).

Sedimentation models in depositional environments establish that siderite ( $\text{FeCO}_3$ ) is

always the first major carbonate to precipitate from ferriferous solutions, because it is the most insoluble of the major common carbonates; whereas minnesotaite ( $\text{Fe}_3\text{Si}_4\text{O}_{10}(\text{OH})_2$ ), a phyllosilicate compositionally close to greenalite, is the simplest of the possible ferrous silicates, as well as a stable phase in terrestrial sediments. According to the reactivity of siderite and minnesotaite given by their corresponding dissociation constants<sup>29</sup>, the equations governing the limits of the stability fields for both minerals with respect to oceanic pH are  $\text{pH} = 3.97 - 0.5 \log p_{\text{CO}_2} - 0.5 \log a_{\text{Fe}^{2+}}$  and  $\text{pH} = 5.1 - 0.5 \log a_{\text{Fe}^{2+}}$ , respectively, for amorphous precipitates.

The combination of pH, redox potential and concentration of  $\text{CO}_2$  determines the stability of carbonates as possible phases, and their precipitation by inorganic processes depends on the saturation state of the solution with respect to these minerals. Oceanic pH specifically related to an equilibrium between aqueous iron and siderite can be determined from the relation  $\log K = \log a_{\text{Fe}^{2+}} + \log p_{\text{CO}_2} - 2 \log a_{\text{H}^+}$ , as calculated in Fig. 1a. Using values at 273 K and a mean concentration for  $\text{Fe}^{2+}$  in sea water of between 50 and 800  $\mu\text{M}$ , a pH between 5.3 and 6.2 for the siderite- $\text{Fe}^{2+}$  equilibrium is obtained for an ocean that occurs in assumed atmospheric  $\text{CO}_2$  pressures of between 0.8 and 4 bar, contrasting to the pH value in modern oceans on Earth, about 8.1; when iron finally photooxidized to  $\text{Fe}^{3+}$ , pH varies between 1.9 and 2.1. Assuming silica concentrations close to the saturation point of oceanic waters on Earth (180  $\mu\text{M}$ , ref. 30) or even higher for water on early Mars (1 mM, ref. 8), and assuming that no Earth-like biological recycling occurred on Mars during the Noachian period, these relations define the boundaries for siderite, minnesotaite, haematite and jarosite precipitation shown in Fig. 1. System evolution over time, coupled to an increased concentration of  $\text{H}_2\text{SO}_4$  with  $\text{Fe}^{3+}$ , which would favour the precipitation of ferric sulphate, is shown in Fig. 2. For the conservative constraints assumed here (see Table 1), neither precipitation nor the metastability of siderite are noted. Increasing the assumed values will result in even more acidic conditions, thus making carbonate formation even less likely. Following the established model for the Earth, additional powerful contributors to the acidity of the Noachian oceans may have been volcanic sulphur-rich gases causing acid rain, as indicated in Fig. 3.

Received 7 January; accepted 23 July 2004; doi:10.1038/nature02911.

- Clifford, S. M. & Parker, T. J. The evolution of the martian hydrosphere: Implications for the fate of a primordial ocean and the current state of the northern plains. *Icarus* **154**, 40–79 (2001).
- Phillips, R. J. *et al.* Ancient geodynamics and global-scale hydrology on Mars. *Science* **291**, 2587–2591 (2001).
- Dohm, J. M. *et al.* Ancient drainage basin of the Tharsis region, Mars: Potential source for outflow channel systems and putative oceans or paleolakes. *J. Geophys. Res.* **106**, 32943–32958 (2001).
- Craddock, R. A. & Howard, A. D. The case for rainfall on a warm, wet early Mars. *J. Geophys. Res.* **107**, doi:10.1029/2001JE001505 (2002).
- Fairén, A. G. *et al.* Episodic flood inundations of the northern plains of Mars. *Icarus* **165**, 53–67 (2003).
- Malin, M. C. & Edgett, K. S. Evidence for persistent flow and aqueous sedimentation on early Mars. *Science* **302**, 1931–1934 (2003).
- Moore, J. M. Blueberry fields for ever. *Nature* **428**, 711–712 (2004).
- Catling, D. C. A chemical model for evaporites on early Mars: Possible sedimentary tracers of the early climate and implications for exploration. *J. Geophys. Res.* **104**, 16453–16469 (1999).
- Bandfield, J. L., Glotch, T. D. & Christensen, P. R. Spectroscopic identification of carbonate minerals in the martian dust. *Science* **301**, 1084–1087 (2003).
- Carr, M. H. & Head, J. W. Oceans on Mars: An assessment of the observational evidence and possible fate. *J. Geophys. Res.* **108**, doi:10.1029/2002JE001963 (2003).
- Kirkland, L. E., Herr, K. C. & Adams, P. M. Infrared stealthy surfaces: Why TES and THEMIS may miss some substantial mineral deposits on Mars and implications for remote sensing of planetary surfaces. *J. Geophys. Res.* **108**, doi:10.1029/2003JE002105 (2003).
- Huguenin, R. L. J. The formation of goethite and hydrated clay minerals on Mars. *J. Geophys. Res.* **79**, 3895–3905 (1974).
- Mukhin, L. M., Koscheev, A. P., Dikov, Yu. P., Huth, J. & Wänke, H. Experimental simulations of the photo-decomposition of carbonates and sulphates on Mars. *Nature* **379**, 141–143 (1996).
- Clark, B. C. On the non-observability of carbonates on Mars. *5th Mars Conf. Abstr.* 6214 (Lunar and Planetary Institute, Houston, Texas, 1999).
- Baker, V. R. Water and the Martian landscape. *Nature* **412**, 228–236 (2001).
- Head, J. W. III, Kreslavsky, M. A. & Pratt, S. Northern lowlands of Mars: Evidence for wide-spread volcanic flooding and tectonic deformation in the Hesperian Period. *J. Geophys. Res.* **107**, doi:10.1029/2000JE001445 (2002).
- Bhattacharyya, A. & Friedman, G. M. *Modern Carbonate Environments* (Hutchinson Ross, Stroudsburg, Pennsylvania, 1983).
- Brain, D. A. & Jakosky, B. M. Atmospheric loss since the onset of the martian geologic record: Combined role of impact erosion and sputtering. *J. Geophys. Res.* **103**, 22689–22694 (1998).
- Squyres, S. W. & Kasting, J. F. Early Mars: How warm and how wet? *Science* **265**, 744–749 (1994).
- Forget, F. & Pierrehumbert, R. T. Warming early Mars with carbon dioxide clouds that scatter infrared radiation. *Science* **278**, 1273–1276 (1997).
- Melosh, H. J. & Vickery, A. M. Impact erosion of the primordial atmosphere of Mars. *Nature* **338**, 487–489 (1989).
- Barley, M. E., Pickard, A. L. & Sylvester, P. J. Emplacement of a large igneous province as possible cause of banded iron formation 2.45 billion years ago. *Nature* **385**, 55–58 (1997).
- Russell, M. J. & Hall, A. J. The emergence of life from iron monosulphide bubbles at a submarine hydrothermal redox and pH front. *J. Geol. Soc.* **154**, 377–402 (1997).
- Holland, H. D. The oceans: A possible source of iron in iron-formations. *Econ. Geol.* **68**, 1169–1172 (1973).
- Zuber, M. T. The crust and mantle of Mars. *Nature* **412**, 220–227 (2001).
- Schaefer, M. W. Aqueous geochemistry on early Mars. *Geochim. Cosmochim. Acta* **57**, 4619–4625 (1993).
- Burns, R. G. Ferric sulfates on Mars. *J. Geophys. Res.* **92**, 570–574 (1987).
- Fernández-Remolar, D. *et al.* The Tinto river, an extreme acidic environment under control of iron, as an analog of the *Terra Meridiani* hematite site of Mars. *Planet. Space Sci.* **52**, 239–248 (2003).

- Johnson, J. W., Oelkers, E. H. & Helgeson, H. C. SUPCRT92: A software package for calculating the standard molal thermodynamic properties of minerals, gases, aqueous species, and reactions from 1 to 5000 bars and 0° to 1000 °C. (Earth Sciences Department, Lawrence Livermore Laboratory, 1991).
- Bruland, K. W. in *Chemical Oceanography* 8 (eds Riley, J. P. & Chester, R.) 157–220 (Academic, London, 1983).

**Acknowledgements** Special acknowledgements to the MER team, as their compelling evidence probing the acidity of martian palaeoenvironments was unfolded while our work was in progress, and resulted in adjustments in our model following our initial submitted draft. We also thank S. Clifford, I. Fairchild and J. Kasting for comments and suggestions that refined and focused this paper.

**Competing interests statement** The authors declare that they have no competing financial interests.

**Correspondence** and requests for materials should be addressed to A.G.F. (agfai@cbm.uam.es).

## A high-intensity highly coherent soft X-ray femtosecond laser seeded by a high harmonic beam

Ph. Zeitoun<sup>1</sup>, G. Faivre<sup>1</sup>, S. Sebban<sup>1</sup>, T. Mocek<sup>1</sup>, A. Hallou<sup>1</sup>, M. Fajardo<sup>2</sup>, D. Aubert<sup>3</sup>, Ph. Balcou<sup>1</sup>, F. Burgy<sup>1</sup>, D. Douillet<sup>1</sup>, S. Kazamias<sup>4</sup>, G. de Lachèze-Murel<sup>3</sup>, T. Lefrou<sup>1</sup>, S. le Pape<sup>5</sup>, P. Mercère<sup>1</sup>, H. Merdji<sup>6</sup>, A. S. Morlens<sup>1</sup>, J. P. Rousseau<sup>1</sup> & C. Valentin<sup>1</sup>

<sup>1</sup>Laboratoire d'Optique Appliquée, chemin de la Lumière, 91761 Palaiseau, France

<sup>2</sup>Centro de Física dos Plasmas, Instituto Superior Técnico, Avenida Rovisco Pais, 1049-001 Lisboa, Portugal

<sup>3</sup>CEA/DIE, BP 12, 91680 Bruyères-le-châtel, France

<sup>4</sup>Laboratoire d'Interaction du Rayonnement X avec la Matière, bâtiment 350, Université Paris-Sud, 91405 Orsay, France

<sup>5</sup>Laboratoire pour l'Utilisation des Lasers Intenses, École Polytechnique, 91128 Palaiseau, France

<sup>6</sup>CEA/SPAM, bâtiment 522, Centre d'Études de Saclay, 91191 Gif-sur-Yvette, France

Synchrotrons have for decades provided invaluable sources of soft X-rays, the application of which has led to significant progress in many areas of science and technology. But future applications of soft X-rays—in structural biology, for example—anticipate the need for pulses with much shorter duration (femtoseconds) and much higher energy (millijoules) than those delivered by synchrotrons. Soft X-ray free-electron lasers<sup>1</sup> should fulfil these requirements but will be limited in number; the pressure on beamtime is therefore likely to be considerable. Laser-driven soft X-ray sources offer a comparatively inexpensive and widely available alternative, but have encountered practical bottlenecks in the quest for high intensities. Here we establish and characterize a soft X-ray laser chain that shows how these bottlenecks can in principle be overcome. By combining the high optical quality available from high-harmonic laser sources (as a seed beam) with a highly energetic soft X-ray laser plasma amplifier, we produce a tabletop soft X-ray femtosecond laser operating at 10 Hz and exhibiting full saturation, high energy, high coherence and full polarization. This technique should be readily applicable on all existing laser-driven soft X-ray facilities.

A laser chain consists of several stages: a seed oscillator, delivering a pulse of perfect optical properties, followed by amplifiers, set to increase beam energy. We studied the extension of this scheme to the soft X-ray range. The main difficulties while designing an amplification chain are first to produce a seed with high optical quality, then to maintain the quality over the amplification stages and finally to reduce the spurious self-emission of the amplifiers to a